

Optimal conditions for observing Josephson oscillations in a double-well Bose-gas condensate

J. E. Williams

Department of Physics, University of Toronto, Toronto, Ontario M5S 1A7, Canada

(Dated: November 6, 2018)

The Josephson oscillations between condensates in a double-well trap are known theoretically to be strongly effected by the mean field interaction in dilute atomic gases. The most important effect is that the amplitude of oscillation in the relative population of the two wells is greatly suppressed due to the mean field interaction, which can make it difficult to observe the Josephson effect. Starting from the work of Raghavan, Smerzi, Fantoni, and Shenoy, we calculate the maximum amplitude of oscillation in the relative population as a function of various physical parameters, such as the trap aspect ratio, the Gaussian barrier height and width, and the total number of atoms in the condensate. We also compare results for ^{23}Na and ^{87}Rb . Our main new result is that the maximum amplitude of oscillation depends strongly on the aspect ratio of the harmonic trap and can be maximized in a “pancake” trap, as used in the experiment of Anderson and Kasevich.

PACS numbers: 03.75.Fi. 05.30.Jp 32.80.Pj

I. INTRODUCTION

In this paper we consider a Bose-Einstein condensate (BEC) at zero temperature trapped in a double-well potential, which is created by superimposing a harmonic trap and a Gaussian barrier. With a finite barrier height that is greater than the condensate chemical potential, the Gross-Pitaevskii dynamics of the condensate can be well described as a superposition of right and left localized condensates, the so-called two-mode ansatz [1]. The weak link allows Josephson tunneling of condensate atoms between wells when there is a chemical potential difference (or a difference in phases) between the wells.

A double well system was implemented in the experiment described in Ref. [2], where the Gaussian barrier was created by focusing a blue-detuned far-off-resonant light sheet into the center of a magnetic trap. The trap had a “cigar” geometry, that is $\lambda \gg 1$, where we have defined the aspect ratio of the radial and axial trap frequencies $\lambda \equiv \omega_\rho/\omega_z$, which turns out to play an important role in our calculations. In the experiment of Ref. [2], an *infinite* barrier along the z -axis was used to separate two independent condensates of about five million ^{23}Na atoms and then removed to allow the condensates to interfere. In this paper we focus on Josephson tunneling through a *finite* barrier, which was not reported in Ref. [2]. To date, there have been no reports of experimental observations of Josephson tunneling in a double-well trap. Josephson tunneling of a condensate in a one dimensional optical lattice was reported in Ref. [3]. Each well in the array held a condensate of about one thousand ^{87}Rb atoms. The chemical potential offset due to gravity caused the condensates to tunnel out of the wells. A crucial characteristic of the experiment is that the wells had an extremely “pancake” geometry ($\lambda \ll 1$) with $\lambda \approx 0.002$ [3, 4], in contrast to the “cigar” geometry of the trap used in Ref. [2]. A related system of two hyperfine states coupled by applied electromagnetic fields was reported in Refs. [5, 6, 7] for the case of strong cou-

pling. Tunneling in a three-component condensate was reported in Ref. [8].

The double-well tunneling system for a Bose condensate has been treated extensively in the recent theoretical literature [1, 9, 10, 11, 12]. Nonlinear Josephson equations describing the oscillations of the relative population $\eta(t) = (N_1(t) - N_2(t))/N_c$ and phase $\phi(t) = \phi_1(t) - \phi_2(t)$ between the wells have been thoroughly explored [1, 13], and this analysis will be the basis of our paper. Here, the indices 1 and 2 label the left and right wells and $N_c = N_1 + N_2$ is the fixed total condensate population, so that $-1 \leq \eta(t) \leq 1$. A crucial property of this system is that, due to the nonlinear terms in the Josephson equations arising from the mean field interaction, there is a maximum amplitude of oscillation $\eta_{\max} < 1$ less than unity. If the initial population difference $\eta(0) \gtrsim \eta_{\max}$, then very little tunneling occurs, a phenomenon referred to as macroscopic quantum “self-trapping” [1]. The calculations of Ref. [12] were carried out using realistic parameters corresponding to the experiment of Ref. [2], but used a finite barrier height to allow tunneling to occur. An extremely small value of $\eta_{\max} \ll 0.01$ was found, indicating that Josephson oscillations in that system would be very difficult to observe due to experimental error in measuring $\eta(t)$ (which we assume to be of the order of a few percent).

Because of the importance of having clear experimental demonstrations of quantum phase oscillations, we feel it is useful to explore a wider range of physical parameters in order to find optimal conditions for observing Josephson oscillations in a double-well. This is the main purpose of the present paper. The key quantities that determine η_{\max} are the condensate density, the s-wave scattering length a , the atomic mass m , and the coupling strength between wells. In the absence of interactions ($a = 0$), the problem reduces to a simple linear two-level system, so that $\eta_{\max} = 1$. The effect of the mean field interaction can be reduced by reducing the density, scattering length, or the mass. In this paper, we do not vary m or a , but

rather, we consider two types of atoms, ^{23}Na and ^{87}Rb , each with a fixed mass and scattering length. We calculate η_{\max} for a wide range of trap parameters by varying the trap geometry determined by ω_z and ω_ρ , the barrier geometry, and the number of condensate atoms N_c . We find η_{\max} is optimized by making the trap more ‘‘pancake’’ shaped ($\lambda \ll 1$), which has the effect of maximizing the weak link area, while maintaining a sufficiently low condensate density. This result is consistent with the fact that Josephson tunneling was clearly observed in Ref. [3] for an array of wells possessing an extreme ‘‘pancake’’ geometry. This behavior is in contrast to that for a trap with a ‘‘cigar’’ geometry, which minimizes the weak link area and compresses the condensate in two dimensions rather than one, resulting in a greater density.

II. DERIVATION OF MODEL

At zero temperature, the condensate dynamics is well described by the Gross-Pitaevskii (GP) equation

$$i\hbar \frac{\partial \Phi(\mathbf{r}, t)}{\partial t} = [H_0 + gn_c(\mathbf{r}, t)] \Phi(\mathbf{r}, t), \quad (1)$$

where $n_c(\mathbf{r}, t) = |\Phi(\mathbf{r}, t)|^2$ is the condensate density and

$$H_0 = -\frac{\hbar^2}{2m} \nabla^2 + U_{\text{ext}}(\mathbf{r}). \quad (2)$$

Here, the external potential $U_{\text{ext}}(\mathbf{r}) = U_H(\mathbf{r}) + U_B(\mathbf{r})$ is created by superimposing a harmonic trap

$$U_H(\rho, z) = m\omega_z^2(\lambda^2 \rho^2 + z^2)/2, \quad (3)$$

and a Gaussian barrier along the z axis.

$$U_B(z) = U_0 \exp(-z^2/2\sigma^2). \quad (4)$$

In our calculations, we consider a range of values for the trap frequencies ω_z and ω_ρ , the barrier height U_0 and width σ , and the condensate population N_c .

A. Two-mode ansatz

For a barrier height that is sufficiently larger than the condensate chemical potential

$$U_0 > \mu_c, \quad (5)$$

there exist two nearly degenerate stationary solutions of the GP equation

$$[H_0 + gn_c(\mathbf{r})] \Phi_\alpha(\mathbf{r}) = \mu_\alpha \Phi_\alpha(\mathbf{r}), \quad (6)$$

where $n_c(\mathbf{r}) = N_c |\Phi_\alpha(\mathbf{r})|^2$. The index $\alpha = \{S, A\}$ indicates the reflection symmetry along the z -axis, symmetric or antisymmetric, respectively. These solutions satisfy the orthonormality condition $\int d\mathbf{r} \Phi_\alpha(\mathbf{r}) \Phi_\beta(\mathbf{r}) = \delta_{\alpha\beta}$.

Left and right localized states can be formed from these eigenstates $\Phi_1(\mathbf{r}) = [\Phi_S(\mathbf{r}) + \Phi_A(\mathbf{r})]/\sqrt{2}$ and $\Phi_2(\mathbf{r}) = [\Phi_S(\mathbf{r}) - \Phi_A(\mathbf{r})]/\sqrt{2}$, respectively, which are also orthonormal.

In the two-mode approximation, the condensate dynamics is described by the following ansatz solution [1]

$$\Phi(\mathbf{r}, t) = \psi_1(t)\Phi_1(\mathbf{r}) + \psi_2(t)\Phi_2(\mathbf{r}). \quad (7)$$

Here, the complex coefficients $\psi_i(t) = \sqrt{N_i(t)} \exp[i\phi_i(t)]$ are spatially uniform and contain all of the time dependence, while the two states $\Phi_1(\mathbf{r})$ and $\Phi_2(\mathbf{r})$ are localized in the left and right wells, respectively, and contain all of the position dependence. In a more accurate theory, one could account for the slow time evolution of the states $\Phi_i(\mathbf{r})$ due to the mean field interaction since the population $N_i(t)$ in each well evolves in time. If the amplitude of oscillation is relatively small, this can be shown to have a negligible effect [12, 14].

B. Gaussian variational solution

Since we are exploring the parameter space of $\{\omega_z, \omega_\rho, U_0, \sigma, N_c\}$ and must solve (6) many times, it is useful to construct a simplified model solution of the left and right states $\Phi_i(\mathbf{r})$. Several earlier studies have shown that a Gaussian variational solution gives an accurate description of the condensate [15, 16, 17]. We therefore employ this procedure by taking the following ansatz for $\Phi_\alpha(\mathbf{r})$

$$\Phi_\alpha(\mathbf{r}) = C_\alpha e^{-A_\alpha^2 \rho^2} [e^{-B_\alpha^2 (z+z_\alpha)^2} \pm e^{-B_\alpha^2 (z-z_\alpha)^2}]. \quad (8)$$

Here, C_α is a normalization constant given by

$$C_\alpha = \sqrt{\frac{2^{1/2} A_\alpha^2 B_\alpha}{\pi^{3/2} [1 \pm \exp(-2B_\alpha^2 z_\alpha^2)]}}. \quad (9)$$

The three variational coefficients $\{A_\alpha, B_\alpha, z_\alpha\}$ must be determined by minimizing the Gross-Pitaevskii energy functional

$$E(\Phi) = \int d\mathbf{r} \left[\frac{\hbar^2}{2m} |\nabla \Phi|^2 + U_{\text{ext}} |\Phi|^2 + \frac{g}{2} |\Phi|^4 \right] \quad (10)$$

with respect to variations in $\{A_\alpha, B_\alpha, z_\alpha\}$. We note that these coefficients will be different for the symmetric and anti-symmetric states. The Gaussian form of our variational ansatz permits us to evaluate the integral in (10) analytically. However, due to the nonlinear terms in the resulting expression, we carry out the minimization of $E(\Phi)$ numerically. In Section III, we compare the Gaussian variational solution with the full numerical solution of (6) and find qualitative agreement over a wide range of parameters.

C. Equations for the relative phase and population

We substitute the two-mode ansatz (7) into the GP equation (1), multiply by $\Phi_i(\mathbf{r})$ and integrate over position to obtain equations of motion for the complex coefficients $\psi_i(t)$ [1]

$$i\hbar\dot{\psi}_i(t) = [E_i + U_i N_i(t)]\psi_i(t) - [K + U_{1,12}N_1(t) + U_{2,12}N_2(t)]\psi_j(t), \quad (11)$$

where we have used the orthonormality property. Here, E_i is the bare zero-point energy in well i ,

$$E_i = \int d\mathbf{r} \Phi_i(\mathbf{r}) H_0 \Phi_i(\mathbf{r}) \quad (12)$$

and $U_i N_i(t)$ is the mean-field interaction energy, with

$$U_i = g \int d\mathbf{r} \Phi_i^4(\mathbf{r}). \quad (13)$$

The term K in (11) is the coupling energy between condensates due to the finite probability of tunneling through the barrier,

$$K = - \int d\mathbf{r} \Phi_1(\mathbf{r}) H_0 \Phi_2(\mathbf{r}). \quad (14)$$

In (11), we also include the mean-field contribution to the coupling, given by $[U_{1,12}N_1(t) + U_{2,12}N_2(t)]$, where

$$U_{i,12} = -g \int d\mathbf{r} \Phi_i^2(\mathbf{r}) \Phi_1(\mathbf{r}) \Phi_2(\mathbf{r}). \quad (15)$$

As shown recently in Ref. [18], these factors (15) give rise to a time-dependent coupling term, but were neglected in the calculation of Ref. [1]. The integrals in (12)-(15) can be carried out analytically using the Gaussian variational solution (8).

It is straightforward to obtain the equations of motion for the phases and populations of each condensate by substituting $\psi_i(t) = \sqrt{N_i(t)} e^{i\phi_i(t)}$ into (11),

$$\dot{N}_i(t) = \frac{1}{\hbar} [U_{1,12}N_1(t) + U_{2,12}N_2(t) + K] [N_i(t)N_j(t)]^{1/2} \sin[\phi_i(t) - \phi_j(t)] \quad (16)$$

$$\hbar\dot{\phi}_i(t) = -E_i - U_i N_i(t) + [U_{1,12}N_1(t) + U_{2,12}N_2(t) + K] \left(\frac{N_j(t)}{N_i(t)} \right)^{1/2} \cos[\phi_i(t) - \phi_j(t)]. \quad (17)$$

Using (16) and (17), we can derive two equations for the relative phase $\phi(t) = \phi_1(t) - \phi_2(t)$ and the relative population $\eta(t) = [N_1(t) - N_2(t)]/N_c$ [1]

$$\dot{\eta}(t) = \omega_J(t) \sqrt{1 - \eta^2(t)} \sin \phi(t), \quad (18)$$

$$\dot{\phi}(t) = -\Delta\omega - \omega_C \eta(t) - \omega_J(t) \frac{\eta(t) \cos \phi(t)}{\sqrt{1 - \eta^2(t)}}, \quad (19)$$

Here we have simplified the notation by defining the Josephson frequency

$$\omega_J(t) \equiv [2K + N_c U_{1,12}(1 + \eta(t)) + N_c U_{2,12}(1 - \eta(t))]/\hbar, \quad (20)$$

the ‘‘capacitive’’ frequency proportional to the mean field interaction

$$\omega_C \equiv N_c(U_1 + U_2)/2\hbar, \quad (21)$$

and the frequency due to the difference in zero-point energies

$$\Delta\omega \equiv [E_1 - E_2 + (U_1 - U_2)N_c/2]/\hbar. \quad (22)$$

For simplicity, we restrict our calculations to a symmetric double-well, since the overall behavior of η_{\max} does not depend much on a relative offset in the well depths. In this case, the spatially averaged quantities (12), (13), and (15) are equal for each well ($E_1 = E_2$, $U_1 = U_2$, $U_{1,12} = U_{2,12} \equiv U_{12}$), allowing us to make the simplifications $\Delta\omega = 0$ and

$$\omega_J = 2(K + N_c U_{12})/\hbar, \quad (23)$$

which is now time-independent. Using these results, the equations of motion (18) and (19) reduce to

$$\dot{\eta}(t) = \omega_J \sqrt{1 - \eta^2(t)} \sin \phi(t), \quad (24)$$

$$\dot{\phi}(t) = -\omega_C \eta(t) - \omega_J \frac{\eta(t)}{\sqrt{1 - \eta^2(t)}} \cos \phi(t). \quad (25)$$

In Ref. [1], Raghavan *et al.* give an analytic solution of (24) and (25) in terms of Jacobian elliptic functions. The solution depends on the initial conditions for the relative number and phase, $\eta(0)$ and $\phi(0)$. From the solution for $\eta(t)$ we can define two maximum amplitudes of oscillation, one for the case $\eta(0) = 0$, the other in the case of a finite $\eta(0) \neq 0$. For equal populations initially, i.e. $\eta(0) = 0$, the maximum amplitude of oscillation η_{\max} can be obtained from equation (B5a) of Ref. [1] by taking $\phi(0) = \pi/2$, which gives

$$\eta_{\max} = \frac{1}{\Lambda} \left[2(\sqrt{\Lambda^2 + 1} - 1) \right]^{1/2}, \quad (26)$$

where $\Lambda \equiv \omega_C/\omega_J$. In the non-interacting limit ($g = 0$), $\omega_C = 0$ and hence $\Lambda = 0$, so that (26) gives $\eta_{\max} = 1$, as it must in this limit. In the strongly interacting limit $\Lambda \gg 1$, (26) takes the approximate form $\eta_{\max} \approx \sqrt{2(\Lambda - 1)}/\Lambda \ll 1$. If instead the initial population difference is nonzero, then a slightly higher amplitude η_c can be obtained compared to that given in (26). Taking $\phi(0) = 0$ in equation (4.9) of Ref. [1], we obtain

$$\eta_c = 2\sqrt{\Lambda - 1}/\Lambda. \quad (27)$$

If $\eta(0) > \eta_c$, then the solution is self-trapped. We note that in the strongly interacting limit $\Lambda \gg 1$, these two

quantities are approximately equal and satisfy the following relation $\eta_c \simeq \sqrt{2}\eta_{\max}$. We work with η_{\max} in our calculations rather than η_c because (26) is valid over the whole range of values for Λ .

For small-amplitude oscillations, (24) and (25) can be linearized and combined to give

$$\ddot{\eta}(t) + \omega_J(\omega_C + \omega_J)\eta(t) = 0. \quad (28)$$

This equation tells us that the system oscillates at the ‘‘Josephson plasma’’ frequency

$$\omega_{\text{JP}} = \sqrt{\omega_J(\omega_C + \omega_J)}. \quad (29)$$

In the case where the mean field interaction is large compared to the coupling energy $\omega_C/\omega_J \gg 1$, this reduces to $\omega_{\text{JP}} = \sqrt{\omega_J\omega_C}$. Due to the mean field interaction, the actual frequency of oscillation between the two wells can be large $\omega_{\text{JP}} > \omega_z$, even though the coupling is weak $\omega_J < \omega_z$.

D. Illustration of nonlinear oscillations

It is instructive to show the time evolution of $\eta(t)$ in order to visualize the behavior of the nonlinear Josephson oscillations and to clarify the precise meaning of η_{\max} , η_c , and ω_{JP} . In Fig. 1 we graph $\eta(t)$ for three different initial conditions $\eta(0)$ and $\phi(0)$ for the solution of the coupled nonlinear equations (24) and (25). We first consider the case of equal populations $\eta(0) = 0$ and an initial relative phase of $\phi(0) = \pi/2$, shown by the solid line. The population difference $\eta(t)$ oscillates with an amplitude of η_{\max} . In the non-interacting limit (eg. $\omega_C \rightarrow 0$), the problem reduces to a linear coupled two-level system and a complete population transfer between wells would occur in this case, $\eta_{\max} = 1$, at a frequency of ω_J . The amplitude suppression introduced by the mean field interaction arises from the term $-\omega_C\eta(t)$ in (25), which acts as a time-dependent offset in the zero-point energies of the two wells. We also indicate the period of small-amplitude oscillation $T_{\text{JP}} \equiv 2\pi/\omega_{\text{JP}}$ on the graph, which is valid when the amplitude is much less than η_{\max} (we have verified this in calculations not shown here). T_{JP} gives a useful estimate of the period, which, in general, depends on the initial conditions.

We also consider the case of unequal initial populations $\eta(0) \neq 0$. For the dashed line in Fig. 1, we have taken $\eta(0) = 0.9\eta_c$ and $\phi(0) = 0$, where the critical amplitude is $\eta_c = 0.11$ for this case. If the initial population difference is larger than η_c , then the population becomes ‘‘trapped’’, as shown for the case of $\eta(0) = 0.15$ by the dot-dashed line. It is important to realize that in the non-interacting limit ($\omega_C \rightarrow 0$), this self-trapping does not occur. In the absence of interactions, a full oscillation of the dot-dashed line would occur between $\eta = \pm 0.15$, at a frequency of ω_J . We remark that for $\eta(0) \approx \eta_c$, higher harmonics appear in the solution due to the non-linearity [1]. We refer the reader to Ref. [1] for a more

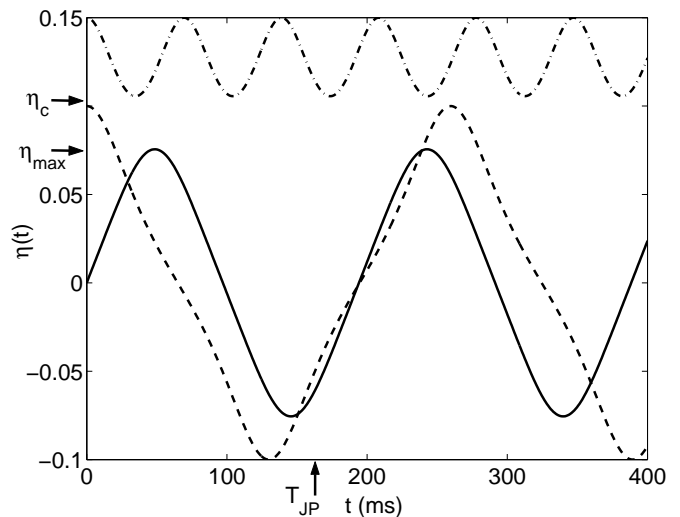


FIG. 1: Amplitude-suppressed Josephson oscillations of $\eta(t)$. The nonlinear equations (24) and (25) for $\eta(t)$ and $\phi(t)$ are solved for different initial conditions: $\eta(0) = 0$, $\phi(0) = \pi/2$ (solid), $\eta(0) = 0.1$, $\phi(0) = 0$ (dashed), $\eta(0) = 0.15$, $\phi(0) = 0$ (dot-dashed). We indicate along the vertical axis the critical value $\eta_c = 0.11$ and the maximum amplitude $\eta_{\max} = 0.075$ obtained when $\eta(0) = 0$. Along the horizontal axis we also indicate the estimated period of the Josephson oscillations $T_{\text{JP}} \equiv 2\pi/\omega_{\text{JP}}$. The physical parameters used correspond to the trap of Ref. [2] in Table 1, but for $N_c = 1000$ atoms.

detailed discussion of this system, where a full range of solutions of (24) and (25) is explored. We also note that this same behavior is also found in Ref. [14] for a condensate with two internal states coupled by a weak external electromagnetic field.

III. RESULTS

In this section we calculate η_{\max} as given by (26) as a function of the trap frequencies $\omega_z/2\pi$ and $\omega_\rho/2\pi$, the barrier height U_0 and width σ , and the condensate population N_c . To do this, we solve for the left and right localized states $\Phi_i(\mathbf{r})$ and then calculate the quantities (12)-(15), so that the frequencies ω_J and ω_C can then be computed. We compare two different solutions of $\Phi_i(\mathbf{r})$, a direct numerical solution [19] of the stationary GP equation (6) and the Gaussian variational ansatz (8). The variational coefficients $\{A_\alpha, B_\alpha, z_\alpha\}$ are computed numerically by minimizing the energy functional $E(\Phi)$ (10) using the Nelder-Mead simplex search algorithm in the software package MATLAB.

While varying the physical parameters ω_z , ω_ρ , σ , and N_c in our calculations, we keep U_0 at a fixed height relative to the chemical potential μ_S , which also varies. The bottom of the double well U_{\min} is obtained by minimizing U_{ext} along the z -axis to give

$$U_{\min} = m\omega_z^2\sigma^2[1 - \ln(m\omega_z^2\sigma^2/U_0)]. \quad (30)$$

TABLE I: Table of trap parameters. In the calculation of η_{\max} , we take $N_c = 10^4$, $\chi = 1.5$, and $\sigma = 1\mu\text{m}$. For the scattering lengths of ^{23}Na and ^{87}Rb , we take $a_{\text{Na}} = 3\text{ nm}$ and $a_{\text{Rb}} = 5.7\text{ nm}$.

trap	$\omega_z/2\pi$ (Hz)	$\omega_\rho/2\pi$ (Hz)	λ	atom	η_{\max}
Ref. [2]	19	250	13	^{23}Na	0.036
Ref. [6]	65	24	0.37	^{87}Rb	0.14
Ref. [7]	8	8	1	^{87}Rb	0.26
Ref. [3]	7200	17	0.002	^{87}Rb	0.85

In our calculations, we define the ratio χ of the barrier height U_0 to the chemical potential μ_S of the symmetric solution, each measured relative to the bottom of the well

$$\chi = \frac{(U_0 - U_{\min})}{(\mu_S - U_{\min})}. \quad (31)$$

We emphasize that in *all* of our calculations, the coupling due to tunneling is *weak*, with $0.05 \lesssim \omega_{\text{JP}}/\omega_z \lesssim 0.5$.

We first calculate η_{\max} for a few typical magnetic traps shown in Table 1. For the ‘‘cigar’’ trap of Ref. [2], taking $N_c = 5 \times 10^6$ and a barrier width of $\sigma = 6\mu\text{m}$, the maximum amplitude of oscillation is miniscule $\eta_{\max} = 5.2 \times 10^{-6}$. Even if we greatly reduce the condensate density by lowering the population $N_c = 10^4$ and increase the coupling by reducing the barrier width $\sigma = 1\mu\text{m}$, the maximum amplitude is still very small, with $\eta_{\max} = 0.036$. The Josephson oscillations would not be visible in this case if the experimental error in measuring η_{\max} were a few percent. For the ‘‘pancake’’ trap of Ref. [6], taking a modest condensate population $N_c = 10^4$ and a narrow barrier $\sigma = 2\mu\text{m}$, we find $\eta_{\max} = 0.054$. A better result can be obtained by decreasing the barrier width $\sigma = 1\mu\text{m}$, which gives $\eta_{\max} = 0.14$. Finally, we consider the spherical trap of Ref. [7], which is a much shallower trap than the other two, so that the density of the condensate is much less. Taking $N_c = 10^4$ and $\sigma = 2\mu\text{m}$, we find $\eta_{\max} = 0.12$, and for $\sigma = 1\mu\text{m}$, $\eta_{\max} = 0.26$. For the optimistic parameters of this shallow trap, Josephson oscillations should be observable.

For comparison we also consider the experimental setup of Ref. [3], where a condensate was loaded into a one dimensional optical lattice. Each well in the array can be modeled as being harmonic as a first approximation, for which one obtains $\omega_z/2\pi \sim 7200\text{ Hz}$ and $\omega_\rho/2\pi \sim 17\text{ Hz}$ [3, 4]. For a rough comparison, we consider a double well with this geometry. Taking $\chi = 1.5$, $\sigma = 1\mu\text{m}$, and $N_c = 10^4$ ^{87}Rb atoms, we find $\eta_{\max} = 0.85$. This value increases to $\eta_{\max} = 0.99$ if we reduce the population to $N_c = 10^3$.

Motivated by these results, we obtain a very crude estimate of the scaling of η_{\max} with the parameters. In the strongly interacting limit $\Lambda \gg 1$, (26) reduces to

$$\eta_{\max} \sim \frac{1}{\sqrt{\Lambda}} \sim \sqrt{\frac{\omega_J}{\omega_C}}. \quad (32)$$

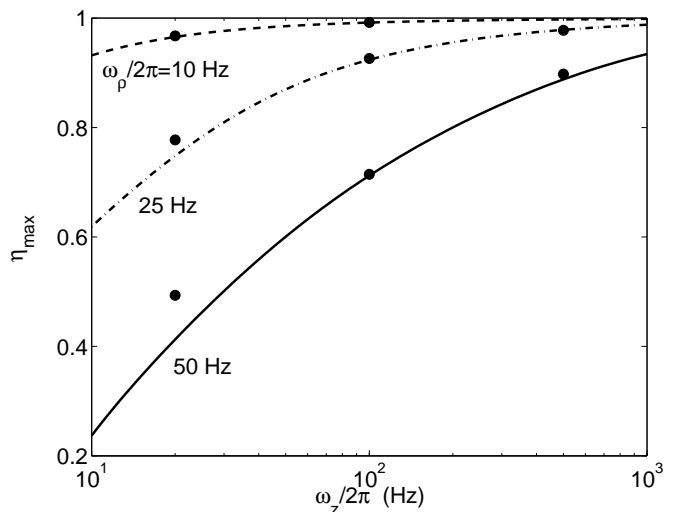


FIG. 2: η_{\max} as a function of $\omega_z/2\pi$ for three values of $\omega_\rho/2\pi$. The three lines are obtained using the Gaussian variational solution (8) and the filled circles are obtained from a full numerical solution of the GP equation (6). In this calculation, the condensate population is held fixed at $N_c = 10^3$ atoms of ^{23}Na . The relative barrier height (31) and width as given in (4) are fixed at $\chi = 1.5$ and $\sigma = 1\mu\text{m}$, respectively.

Taking a simple WKB approach to calculate the tunneling probability [11, 20], an approximate scaling of the Josephson frequency can be obtained $\omega_J/\omega_z \sim \exp[-\sqrt{m\sigma^2(U_0 - \mu)/\hbar^2}]$. One can also get the approximate scaling of ω_C on m and a by taking $\omega_C \sim \mu_{\text{TF}}$, where $\mu_{\text{TF}}/\hbar\omega_z = 0.5[15\lambda^2 N_c a/z_{\text{ho}}]^2/5$ is the chemical potential of a condensate in a harmonic trap in the Thomas-Fermi limit [21]. Inserting the definition of the oscillator length, $z_{\text{ho}} = \sqrt{\hbar/m\omega_z}$, the expression can be simplified to $\omega_C/\omega_z \sim (ma^2 N_c^2 \lambda^4 \omega_z/\hbar)^{1/5}$. Inserting these crude estimates of ω_J and ω_C into (32), we find that η_{\max} scales like

$$\eta_{\max} \sim \frac{\exp[-\sqrt{m\sigma^2(U_0 - \mu)/4\hbar^2}]}{(ma^2 \lambda^4 N_c^2 \omega_z/\hbar)^{1/10}}. \quad (33)$$

This indicates that the amplitude of oscillation can be increased by decreasing m , a , N_c , σ , or U_0 . For a fixed ω_z , η_{\max} increases as λ is decreased, while for a fixed aspect ratio λ , η_{\max} decreases when the trap is tightened by increasing ω_z . Expression (33) only gives a very crude estimate of the scaling behavior. In the following discussion, we explore the dependence of η_{\max} on the physical parameters more quantitatively by calculating ω_J and ω_C numerically.

In Figs. 2 - 5 we plot η_{\max} (given by (26)) as a function of the trap geometry (by varying ω_z and ω_ρ), N_c , and the barrier height χ and width σ . In each figure, we show results for the Gaussian variational solution (lines) and the direct numerical solution of the stationary GP equation (6) (filled points). The Gaussian variational so-

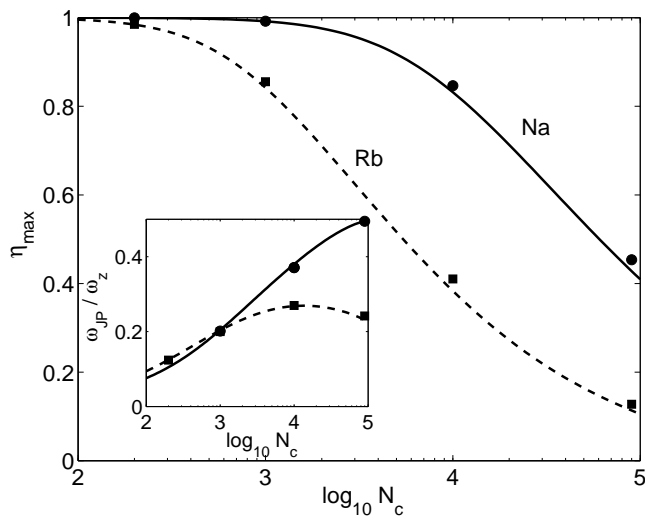


FIG. 3: η_{\max} as a function of the condensate population N_c for ^{23}Na and ^{87}Rb . The lines are obtained using the Gaussian variational solution (8) and the filled circles (^{23}Na) and squares (^{87}Rb) are obtained from a full numerical solution of the GP equation (6). In the inset we show how the frequency of oscillation ω_{JP}/ω_z varies with N_c . In this calculation, the harmonic trap frequencies are held fixed at $\nu_z = 100$ Hz and $\nu_\rho = 10$ Hz. The relative barrier height and width are fixed at $\chi = 1.5$ and $\sigma = 1\mu\text{m}$, respectively.

lution agrees with the full solution within a few percent over a broad range of parameters. The greatest discrepancy occurs in Fig. 2 as ω_z decreases at fixed ω_ρ and in Fig. 4 as σ increases, with the two solutions differing by a factor of 2 at $\sigma = 4\mu\text{m}$ for ^{87}Rb . In all cases, the Gaussian solution slightly underestimates η_{\max} .

Our most important result is shown in Fig. 2, which shows the strong dependence of η_{\max} on the trap geometry. For a fixed value of ω_ρ , η_{\max} can be optimized by increasing the axial trap frequency ω_z , that is, by making the trap more “pancake” like. In contrast, for a fixed value of ω_z , η_{\max} decreases as ω_ρ is increased. It is important to realize that both quantities ω_C and ω_J are effected by changing the aspect ratio of the trap. By making the trap more “pancake” like, one is increasing the area of contact between the two wells, which increases ω_J . On the other hand, compressing the condensate in the z dimension also leads to a higher density, causing ω_C to increase as well. However, the ratio of these two quantities in (32) increases for increasing ω_z . In contrast, by making the trap more “cigar” like, one is decreasing the area of contact between wells, resulting in a decrease in ω_J as ω_ρ increases. Furthermore, in this case one is compressing the condensate in two dimensions rather than one, which results in a more dramatic increase in the density and a corresponding increase in ω_C , so that the ratio ω_J/ω_C decreases with increasing ω_ρ .

In Fig. 3 we vary the condensate population N_c from 10^2 to 10^5 atoms, and show η_{\max} for both ^{23}Na and ^{87}Rb . We see in Figs. 2 - 4 that a much larger amplitude of

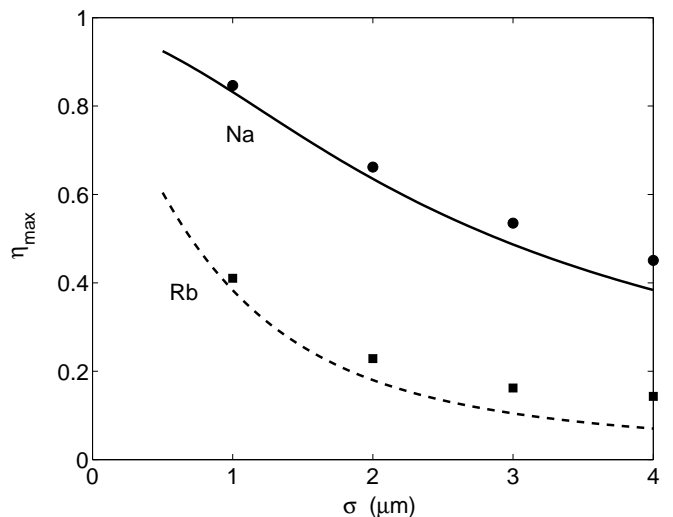


FIG. 4: η_{\max} as a function of the barrier width σ for ^{23}Na and ^{87}Rb . In this calculation, the harmonic trap frequencies are held fixed at $\nu_z = 100$ Hz and $\nu_\rho = 10$ Hz. The relative barrier height is fixed at $\chi = 1.5$ and the population is $N_c = 10^4$ atoms.

oscillation η_{\max} can be achieved using ^{23}Na compared to ^{87}Rb . This behavior is expected based on the rough scaling of η_{\max} given in (33). We can understand why ^{23}Na is favorable over ^{87}Rb , since the mass m of ^{23}Na is about a factor of four smaller than that of ^{87}Rb , and the scattering length a of ^{23}Na is almost half that of ^{87}Rb . As N_c increases in Fig. 3, the effect of the mean field interaction becomes more pronounced causing ω_C to increase, while this has only a small effect on ω_J . We also show the dependence of ω_{JP} on the condensate number N_c in the inset.

We also show the dependence of η_{\max} on the Gaussian barrier parameters by varying the relative height χ (31) in Fig. 4 and the width σ in Fig. 5. We note that varying these two parameters has very little effect on ω_C , which remains roughly constant in these plots. The behavior of η_{\max} is not surprising: as the barrier height and width are each increased, the coupling between wells is diminished so that ω_J decreases, resulting in a decrease in η_{\max} as indicated by (32).

IV. CONCLUSIONS

In this paper we have focussed on an important property of the double-well Josephson system for a dilute atomic Bose-Einstein condensate: the maximum amplitude of oscillation η_{\max} of the population between wells is suppressed due to the mean field interaction [1, 10, 11, 12]. For typical magnetic trap parameters, we have shown that η_{\max} is very small, indicating that Josephson oscillations may be visible only for the very shallow trap used in the experiments described in [7]. We have shown that much larger values of η_{\max} can be achieved by de-

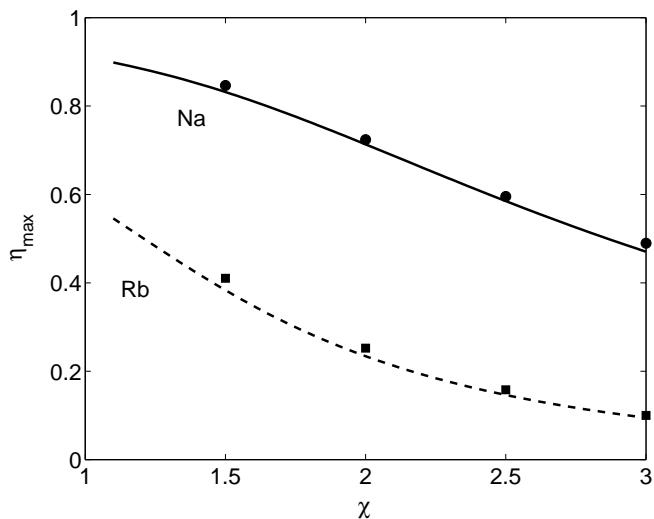


FIG. 5: η_{\max} as a function of the relative barrier height χ defined in (31) for ^{23}Na and ^{87}Rb . In this calculation, the harmonic trap frequencies are held fixed at $\nu_z = 100$ Hz and $\nu_\rho = 10$ Hz. The barrier width is fixed at $\sigma = 1\mu\text{m}$ and the population is $N_c = 10^4$ atoms.

creasing the aspect ratio $\lambda = \omega_\rho/\omega_z$, that is, by making the trap more “pancake” like, in particular, for small val-

ues of the radial frequency ω_ρ . Our study was motivated by the fact that Josephson oscillations were clearly observed in the experiment reported in Ref. [3], where a relatively small condensate was loaded into an array of wells with an extremely small aspect ratio $\lambda \approx 0.002$ [3, 4]. We have also shown that larger values of η_{\max} can be attained by decreasing the condensate population N_c , and decreasing the barrier height χ and width σ . Furthermore, conditions are much more favorable for ^{23}Na compared to ^{87}Rb . It should be noted, however, that present traps for ^{23}Na atoms possess the less optimal “cigar” geometry.

We have restricted our calculations to zero temperature. Our study of the optimal conditions for observing Josephson oscillations should be extended to finite temperatures, where dissipative effects associated with the thermal cloud of non-condensate atoms must be included [11, 22]. Very few explicit calculations of damping rates of Josephson oscillations in a dilute Bose gas have been carried out, and further study of damping in this system is needed.

I would like to thank Prof. A. Griffin for suggesting this problem and for his useful comments. I thank B. Anderson for many insightful comments and E. Zaremba, B. Jackson, and R. Spekkens for useful discussions. This work was supported by a grant from NSERC.

-
- [1] S. Raghavan, A. Smerzi, S. Fantoni, and S. R. Shenoy, Phys. Rev. A **59**(1), 620 (1999).
- [2] M. R. Andrews, C. G. Townsend, H.-J. Miesner, D. S. Durfee, D. M. Kurn, and W. Ketterle, Science **275**(0), 637 (1997).
- [3] B. P. Anderson and M. A. Kasevich, Science **282**, 1686 (1998).
- [4] B. P. Anderson, private communication .
- [5] D. S. Hall, M. R. Matthews, C. E. Wieman, and E. A. Cornell, Phys. Rev. Lett. **81**(8), 1543 (1998).
- [6] M. R. Matthews, B. P. Anderson, P. C. Haljan, D. S. Hall, M. J. Holland, J. E. Williams, C. E. Wieman, and E. A. Cornell, Phys. Rev. Lett. **83**(17), 3358 (1999).
- [7] M. R. Matthews, B. P. Anderson, P. C. Haljan, D. S. Hall, C. E. Wieman, and E. A. Cornell, Phys. Rev. Lett. **83**(13), 2498 (1999).
- [8] H.-J. Miesner, D. M. Stamper-Kurn, J. Stenger, S. Inouye, A. P. Chikkatur, and W. Ketterle, Phys. Rev. Lett. **82**(11), 2228 (1999).
- [9] J. Javanainen, Phys. Rev. Lett. **57**(25), 3164 (1986).
- [10] G. J. Milburn, J. Corney, E. M. Wright, and D. F. Walls, Phys. Rev. A **55**(6), 4318 (1997).
- [11] I. Zapata, F. Sols, and A. J. Leggett, Phys. Rev. A **57**(1), R28 (1998).
- [12] L. Salasnich, A. Parola, and L. Reatto, Phys. Rev. A **60**(5), 4171 (1999).
- [13] I. Marino, S. Raghavan, S. Fantoni, S. R. Shenoy, and A. Smerzi, Phys. Rev. A **60**(1), 487 (1999).
- [14] J. Williams, R. Walser, J. Cooper, E. Cornell, and M. Holland, Phys. Rev. A **59**(1), R31 (1999).
- [15] G. Baym and C. J. Pethick, Phys. Rev. Lett. **76**(1), 6 (1996).
- [16] V. M. Pérez-García, H. Michinel, J. I. Cirac, M. Lewenstein, and P. Zoller, Phys. Rev. Lett. **77**(27), 5320 (1996).
- [17] C. Menotti, J. R. Anglin, J. I. Cirac, and P. Zoller, Phys. Rev. A **66**, 023601 (2001).
- [18] Y. Zhang and H. J. W. Müller-Kirsten, cond-mat/0012491 .
- [19] M. J. Holland, D. S. Jin, M. L. Chiofalo, and J. Cooper, Phys. Rev. Lett. **78**(20), 3801 (1997).
- [20] F. Sols, in *Proceedings of the International School of Physics - Enrico Fermi*, edited by M. Inguscio, S. Stringari, and C. E. Wieman (IOS Press, 1999), p. 453.
- [21] F. Dalfovo, S. Giorgini, L. P. Pitaevskii, and S. Stringari, Rev. Mod. Phys. **71**(3), 463 (1999).
- [22] J. Ruostekoski and D. F. Walls, Phys. Rev. A **58**(1), R50 (1998).